Cu_2S/CdS:Zn heterojunction synthetized by chemical bath deposition for photovoltaic application

H. MOUALKIA[1], L. HERISSI[1,2,*], H. CHERIET[1], D. RECHEM[1], L. REMACHE[1]
[1]*Laboratory of Materials and Structure of Electromechanical Systems and their Reliability, Faculty of exact sciences and natural and life sciences, Larbi Ben M'hidi University, Oum El Bouaghi 04000, Algeria*
[2]*Department of Matter Sciences, Echahid Cheikh Larbi Tebessi University, Tebessa 12000, Algeria*

Copper sulfide (Cu_2S) thin film was deposited on zinc-doped cadmium sulfide (CdS:Zn) entirely produced by chemical bath deposition technique onto transparent indium tin oxide (ITO) coating substrates, using gold as a back contact. Before this, the structural, morphological, and optical properties of undoped and 4 wt % Zn-doped CdS thin films have been investigated. The X-ray diffraction spectra showed that the CdS thin films are polycrystalline nature with preferred growth along (111) orientation and the incorporation of Zn does not change qualitatively the crystalline phase of CdS. Scanning electron microscopy measurements indicated that deposited films are homogeneous. Optical transmittance of the film showed an increasing trend from 76 % in the undoped film to 85 % in 4 wt % Zn-doped film. The optical band gap of CdS is found to decrease from 2.43 eV to 2.37 eV for 4 wt % Zn-doped thin film. The I(V) characteristic of the Cu_2S/CdS:Zn heterojunction was found to be rectifying and the current-voltage measurements revealed an ideality factor (n = 2.3).

(Received June 22, 2024; accepted October 7, 2024)

Keywords: Metal chalcogenides, Chemical bath deposition, Cu_2S/CdS:Zn heterojunction, Ideality factor, Saturation current

1. Introduction

Thin films made of metal chalcogenides have significant optoelectronic properties [1-4]. As a member of metal chalcogenides, copper sulfide (Cu_2S) and cadmium sulfide (CdS) have received much attention in recent time due to their potential applications [5-11]. Chemical bath deposition (CBD) is one of the most commonly used techniques to grow Cu_2S and CdS thin films [12,13]. It's recognized to be a simple, low temperature, and inexpensive large-area deposition technique and a well-established method for preparing bi-layers of two different chalcogenide materials such as PbS-CdS [14], PbS-Cu_xS [15], and CdS/ZnS [16]. Copper sulfide is an important semiconductor acting as p-type material due to the copper vacancies happening within the lattice [17]. Cu_xS has received much attention in recent time due to its potential applications in optical and electrical devices like optical filters [18], photoconductor [19], light emitting diodes [20], photo thermal conversion of solar energy [21], potovoltaic applications [22], and solar radiation absorber [23]. Cadmium sulfide is a wide optical band gap (2.4 eV), CdS shows n-type conductivity due to its native defects or sulfur vacancies and cadmium interstitials. CdS is considered as one of the most favorable and employed materials as window layer/buffer layer in various types of hetero-junction solar cells such as CdS/CIGS [24, 25], Cu_2ZnSnS_4/CdS [26], CdS/Cu_2S [27], Cu_2S/CdS [28], and CdS/Cu_2S [29]. Doping the CdS buffer layer material by Zn enhances the electronic, electrical, and optical properties of devices [30]. Conformity of a Zn into the lattice of CdS can adapt its energy gap and lattice parameters, which make it useful in solar cells and diodes [31]. This study focuses on (1) the structural, morphological and optical properties of undoped CdS, 4 wt % Zn-doped CdS, and Cu_2S thin film grown during 3 hrs and (2) the investigation of current-voltage (I-V) characteristics of the elaborated Cu_2S/CdS:Zn heterojunction structure at room temperature.

2. Experimental details

2.1. Preparation of n-type of CdS:Zn

CdS thin films were prepared on glass substrates by chemical bath deposition technique using standard solutions of cadmium sulfate $CdSO_4$ (1 M), thiourea $CS(NH_2)_2$ (1 M), ammonia NH_4OH (9.5 M) and distilled water (DW). Here, cadmium sulfate and thiourea are the source of Cd^{+2} and S^{-2}. Zinc doping was achieved by adding appropriate amounts of zinc sulfate $ZnSO_4$ (5.7 mM) to the main solution, Zn-doped film was prepared with 4 wt %. Glass substrates were ultrasonically cleaned with acetone and methanol, rinsed with water and dried in hot air. The pH monitored with a digital pH-meter was adjusted at ~11 by addition of ammonia. Then, the glass substrates were vertically immersed in the chemical bath and the temperature was regulated at 60 °C. After deposition (30 min for each deposition), the samples were removed from the reaction solution, washed with water and annealed at 300 °C for 15 min (Fig. 1).

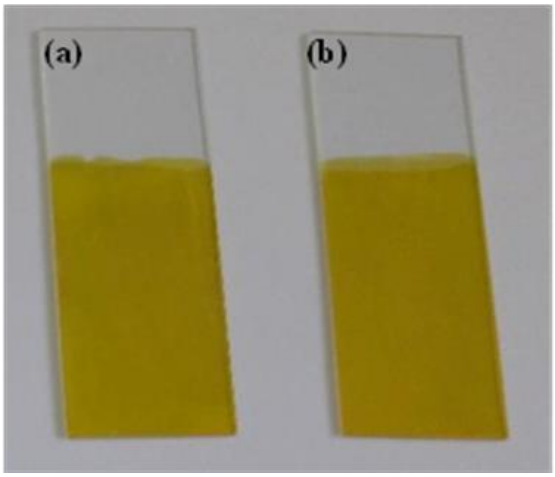

Fig. 1. Images showing the deposited CdS thin films: (a) undoped and (b) 4 wt % Zn-doped CdS thin film (color online)

2.2. Preparation of p-type of Cu_2S

Cu_2S film was deposited by the CBD technique onto glass substrates with dimensions of 4 cm length, 2 cm width and 3 mm thickness. The chemical bath was composed by triethanolamine $C_6H_{15}NO_3$ (50 %), copper (II) chloride dihydrate $CuCl_2{\cdot}2H_2O$ (1 M), ammonia NH_4OH (7.5 M), sodium hydroxide NaOH (1 M), thiourea $CS(NH_2)_2$ (0.5 M) and distilled water (DW). Triethanolamine and sodium hydroxide work as a complexing agent, whereas ammonia solution was used for adjusting pH of the bath solution at alkaline medium (pH = 10.5). During deposition, the solution temperature was kept constant at 37°C. The deposition time was 3 hrs. After deposition, the sample was removed from the reaction solution, washed with distilled water and annealed at 300 °C for 15 min (Fig. 2).

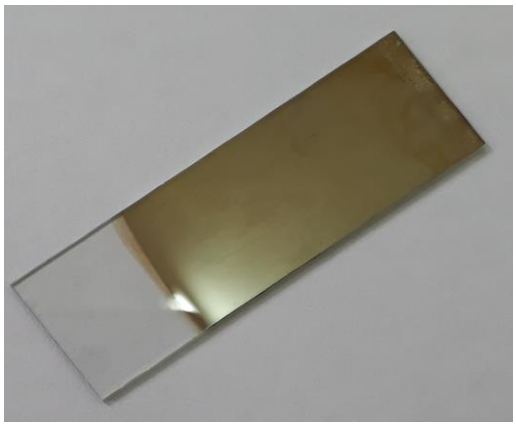

Fig. 2. Images showing the deposited Cu_2S film (color online)

2.3. Preparation of the diode structure (Au/Cu_2S/CdS:Zn/ITO)

The synthesis of the structure **(**Au/Cu_2S/CdS:Zn/ITO**)** is done as follows. First, thin film of CdS:Zn was deposited onto indium doped tin oxide coated conducting glass substrates with the same conditions under which we deposited the CdS:Zn film by chemical bath on a glass substrate (section one). Then, the formed CdS:Zn/ITO thin film is dipped into a second chemical bath which has the same conditions with which we deposited the Cu_2S thin layer (section two). After this, Cu_2S/CdS:Zn/ITO multilayer film deposited was annealed at 300 °C for 15 min. At last, Gold (Au) contact was deposited by electron beam evaporation on Cu_2S layer.

2.4. Characterization

Structural properties of the prepared films were performed by X-rays diffractometer (XRD, Brucker-AXXS, D8) with CuK_α radiation. It can be noted that the values of Bragg's angle (2θ) were varied in a range of 20° and 100°.

The crystallite size can be simply determined using the Scherer formula [32]:

$$D_C = \frac{k\lambda}{\beta \cos\theta} \tag{1}$$

while k is the Scherer constant, its value is taken as 0.9 for the calculations [33], λ is the wavelength of incident radiation (λ = 1.5406 Å), β is the full width at half maximum (FWHM) of the peak corrected for instrumental broadening, and θ is the Bragg angle.

The surface morphology of the films was investigated using a FEG 7600F JEOL scanning electron microscopy (SEM). The grain sizes (Dg) are estimated from the AFM measurements "atomic force microscopy" (A.P.E. Research-A100 AFM). The chemical composition of all samples was carried out using an energy dispersive X-ray microanalysis machine (INCA, XMAX, Oxford Instrument, Oxford, UK).

The optical transmittance was recorded using Jasco V-630 spectrophotometer in the wavelength range 100-1100 nm. The absorption coefficient (α) of CdS, CdS:Zn, and Cu_2S thin films was calculated using the transmittance (T) value and thickness (d) using Beer–Lambert law [34]:

$$\alpha = \frac{1}{d}\ln\left(\frac{1}{T}\right) \tag{2}$$

where the film thickness (d) was measured by fitting the transmittance spectra [35].

The α is related to the optical band gap (E_g) by the Tauc formula [36]:

$$(\alpha h\upsilon)^2 = A\left(h\upsilon - E_g\right) \tag{3}$$

where as $h\upsilon$ is the photon energy of the incident photons, A is a constant.

The current–voltage (I-V) measurement was performed in dark conditions and at room temperature using a KEITHLEY 2410 source meter.

3. Results and discussion

3.1. Properties of undoped and 4 wt % Zn-doped CdS thin films

In Fig. 3, the XRD patterns of undoped and 4 wt % Zn-doped CdS film were reported.

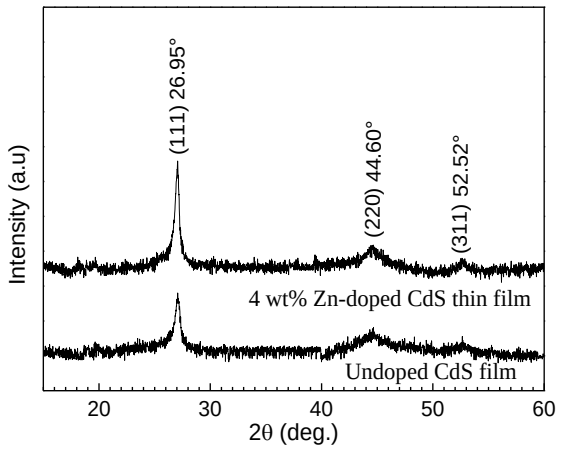

Fig. 3. XRD patterns of undoped and 4 wt% Zn doped CdS films

Table 1. FWHM estimated by X-ray diffraction, crystallite size, thickness and grain size for undoped and 4 wt % Zn-doped CdS thin films.

Thin films type	*FWHM* (deg.)	D_C (nm)	*Thickness* (nm)	*Dg* (nm)
Undoped CdS	0.419	19.5	118	65
4 wt % Zn-doped CdS	0.438	18.7	158	99

It is clearly seen from this figure that different peaks appeared at 2θ = 26.95°, 2θ = 44.3° and 2θ = 52.3°. These peaks correspond respectively to the (111), (220) and (311) planes of the cubic structure in agreement with the JCPDS card No 42-1411 [37]. No peaks for Zn or ZnS were detected which suggests that incorporation of Zn^{+2} ions in the films does not alter the crystalline structure of CdS film. Fig. 4 displays the scanning electron microscopy micrographs of undoped and 4 wt % Zn-doped CdS film. The SEM images show many grains which are homogeneously distributed over the substrate surface. Grain sizes (Dg) are estimated from the AFM measurements (Table 1).

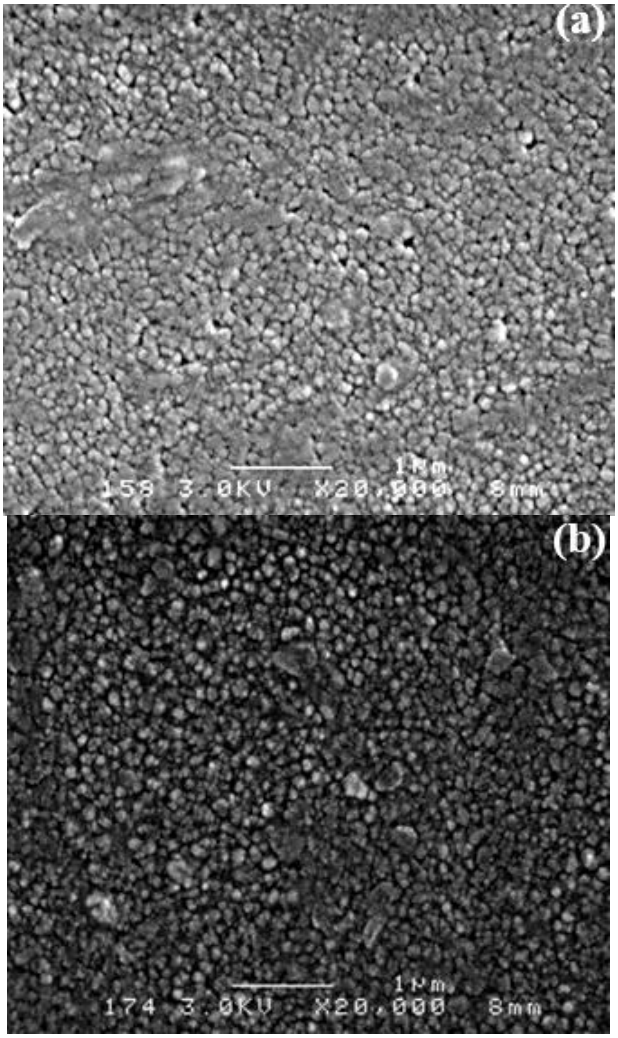

Fig. 4. Scanning electron microscopy (SEM) micrographs of (a) undoped and (b) 4 wt % Zn-doped CdS thin film

Fig. 5(a) and (b) shows the EDAX spectra of undoped and 4 wt % Zn-doped CdS thin film, these spectra exhibit several peaks which are mainly related to Cd and S elements. The spectra of 4 wt % Zn-doped CdS thin film (Fig. 5.b) illustrates other peaks which are assigned to Zn atoms. The supplementary elements (C, Na, Si, O and Mg) may originate from the glass substrates [38]. The weight ratio and atomic ratio compositions of the elements Cd, S, Zn and O for undoped and Zn-doped CdS films are displayed in the insets in Fig. 5.

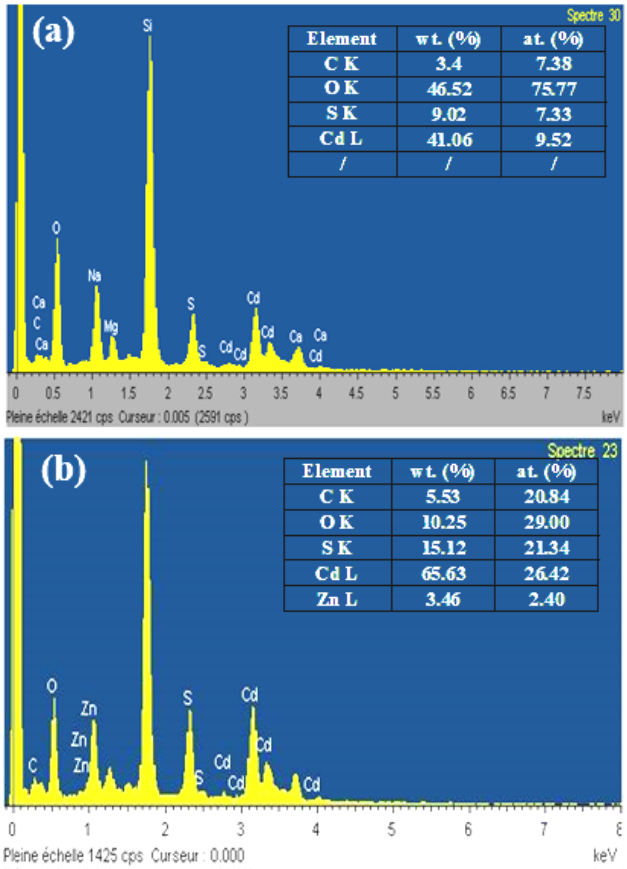

Fig. 5. Energy dispersive X-ray spectroscopy (EDAX) *spectra of (a) undoped CdS thin film and (b) 4 wt % Zn-doped CdS film (color online)*

Fig. 6 shows the optical transmission spectra of undoped and 4 wt % Zn-doped CdS films. As shown in this figure, the films present a high transmittance between 76 and 86 % in the visible and NIR region which is good for optelectronic devices, especially for solar cell window layers. A sharp absorption edge characteristic of CdS which is about 487 nm [39].

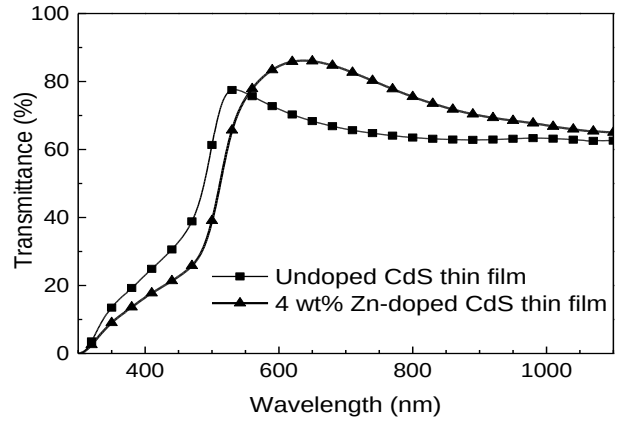

Fig. 6. Transmittance curves of undoped and 4 wt % Zn-doped CdS thin films

The energy band gap value of the undoped and 4 wt % Zn-doped CdS thin films are estimated by plotting $(\alpha h\upsilon)^2$ versus $h\upsilon$ (Fig. 7). Undoped film has a bandgap of 2.43 eV which agrees well with the 2.42 eV bandgap of single crystal CdS [40]. The band gap of 4 wt % Zn-doped thin film is 2.37 eV.

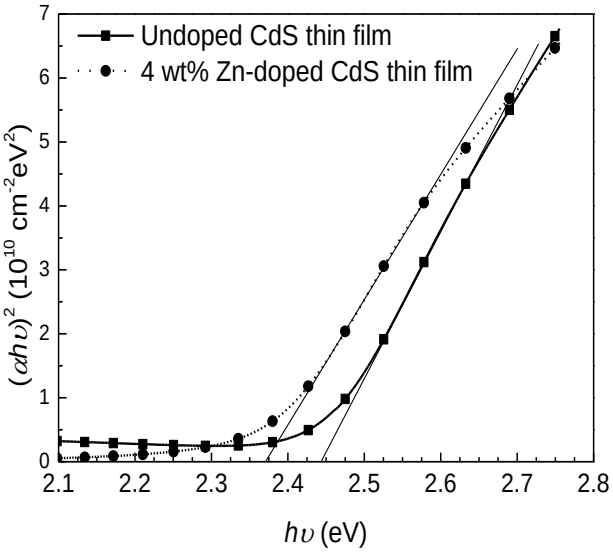

Fig. 7. Plot of $(\alpha h\upsilon)^2$ versus the $h\upsilon$ for the optical band gap determination of undoped and Zn-doped CdS thin film

3.2. Properties of Cu_2S thin film

Fig. 8 shows the X-ray diffraction spectrum of the as-deposited copper sulfide thin film deposited for 3 hrs by chemical bath deposition. At low diffraction angle, we note the presence of halo (or broad) diffraction peak in the form of a bump, located between 20° and 35° is relative to the glass substrate which is amorphous [41]. The diffraction peak centered around 2θ = 46° can be assigned to the (220) crystal planes of Cu_2S which can be indexed as a hexagonal structure. The reported values matched well with the standard JCPDS card No. 03-1071.

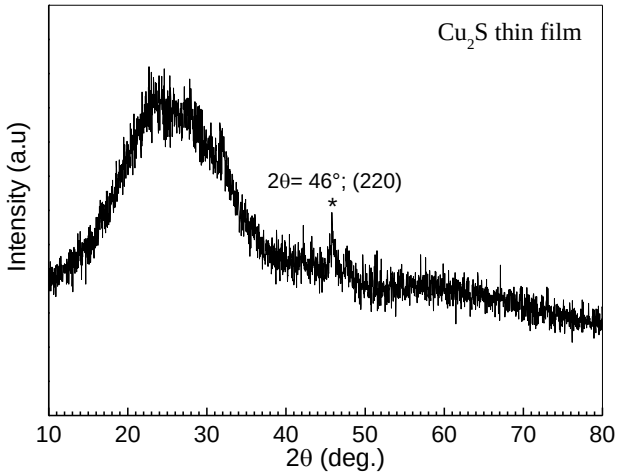

Fig. 8. XRD spectrum of Cu_2S thin film deposited for 3 hours

Fig. 9 shows the scanning electron microscopy micrograph of Cu_2S thin film deposited for 3 hrs. The grain size of this film was much smaller and has complete coverage over the substrate surface. The film is uniform and covers the substrate very well without visible pores. We observe aggregates due to the colloidal particles formed in solution, then adsorbed on the film.

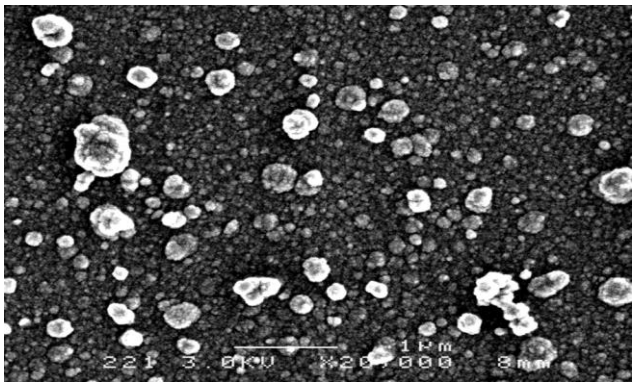

Fig. 9. Scanning electron microscopy (MEB) micrograph *of Cu_2S thin film deposited for 3 hours*

The elemental analysis of the Cu_2S thin film deposited for 3 hrs on glass substrate was investigated by energy dispersive X-ray analysis (EDAX) technique. The EDAX pattern is shown in Fig. 10, peaks of Cu and S exhibit the presence of these elements in the as-deposited film. The peaks of Si, C, Mg and O originate from the glass substrate. We note a high percentage of oxygen, this is due, (i) to the large part of the oxygen comes from the glass substrate which is formed of silica (SiO_2), (ii) to the oxygen comes from the environment.

The elemental analysis was carried out, the insets in Fig. 10 shows elemental weights (wt. %) and atomics (at. %) of Cu and S in the deposited Cu_2S thin film. The average atomic percentage of Cu:S in the as deposited film was calculated as 8.49:5.14.

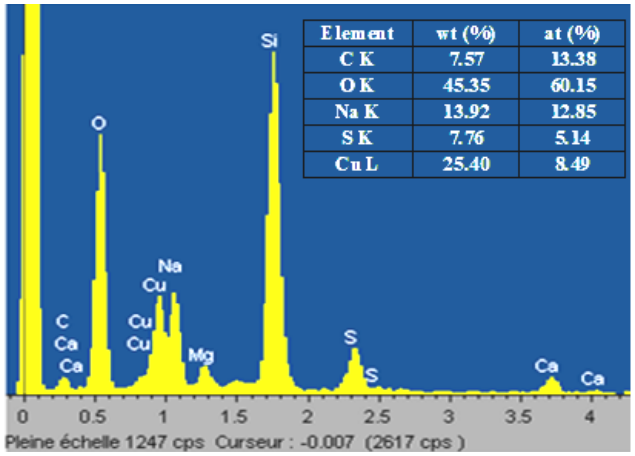

Fig. 10. Energy dispersive X-ray spectroscopy (EDAX) *spectra of Cu_2S thin film deposited for 3 hours (color online)*

The variation of the transmittance and the absorbance of the Cu_2S film as a function of the wavelength is presented in Fig. 11. The transmittance spectrum has a 35 % transparency at 670 nm and decreases slightly with the increase of the wavelength. There is a high absorbance in the wavelength range between 191 and 430 nm, then a decrease in the range 430-700 nm, followed by a slight increase in absorbance beyond 700 nm. It should be noted that copper sulfide is an ideal semiconductor for the absorption of solar energy [42,43], which is why this latter is used in the production of solar cells as an absorber [44]. The thickness of the deposited Cu_2S is 75 nm.

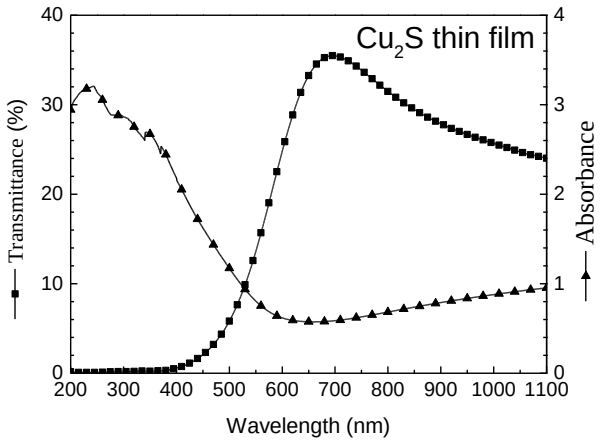

Fig. 11. Variation of the transmittance and the absorbance of Cu_2S thin film as a function of the wavelength.

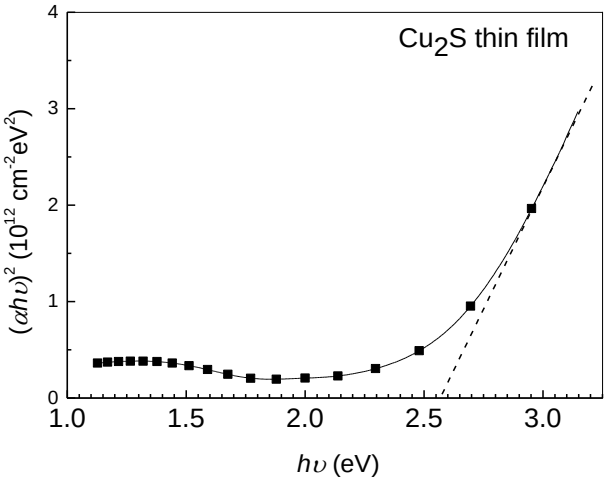

Fig. 12. Plot of $(\alpha h\upsilon)^2$ versus $h\upsilon$ for the optical band gap determination of Cu_2S thin film.

The bandgap was determined by plotting $(\alpha h\upsilon)^2$ versus $h\upsilon$ and then extrapolating the straight line portion to the energy axis (Fig. 12), the estimated Cu_2S thin film direct band gap is 2.6 eV.

3.3. Electrical study of Cu_2S/CdS:Zn heterojunction

3.3.1. Dark current-voltage characteristic

Fig. 13 illustrates the current–voltage (I-V) characteristic of Cu_2S/CdS:Zn heterojunction at room

temperature (300 K) for forward biase voltage. It can be noticed that the current increases exponentially with the increase of the applied bias voltage. Thus the junction was found to be rectifying.

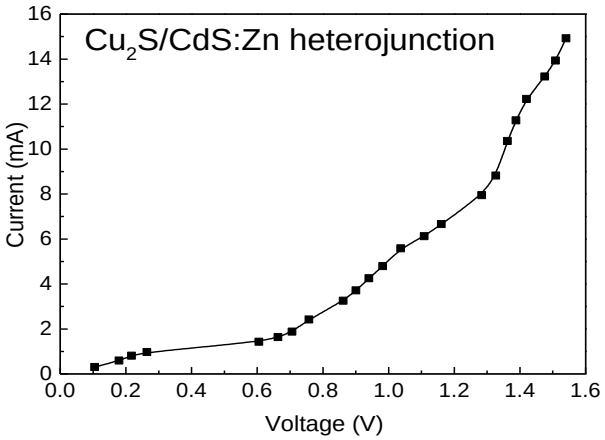

Fig. 13. Current-voltage characteristic of Cu_2S/CdS:Zn heterojunction

The $I(V)$ formulation at forward bias voltage of p-n heterojunction structure can be given by the following expression [40, 45]:

$$I = I_S\left[\exp\left(\frac{qV}{nkT}\right)-1\right] \tag{4}$$

where q is the electron charge, k is the Boltzmann constant, T is the temperature and I_S denotes the saturation current which can be derived from the intersection between the current axis and the interpolated line associated with the first linear region.

The ideality factor (n) is strongly depending on the applied voltage and can be calculated using the following formula [46]:

$$n = \frac{q}{kT}\frac{dV}{d(\ln I)} \tag{5}$$

The saturation current and the ideality factor determined from $I(V)$ characteristic are $4.26\text{x}10^{-4}$ A and 2.3, respectively.

4. Conclusion

In the present work, Cu_2S/CdS:Zn heterojunction thin films have been prepared by chemical bath deposition method. In order to boost the Cu_2S/CdS:Zn heterojunction performance and optimize the experimental conditions, the structural, morphological and optical properties of undoped and 4 wt % Zn-doped CdS thin films properties were investigated. The study indicates that 4 wt % Zn-doped film give the best results. The optimized Cu_2S/CdS:Zn heterojunction shows a good performances and gives low ideality factor and saturation current (2.3 and 4.26×10^{-4} A, respectively) which were prepared by chemical bath deposition can be used to fabricate efficient heterojunctions. This study helps in the evolution of Cu_2S/CdS:Zn heterojunction solar cell. These results suggest that the elaborated device by chemical bath play an important role in fabricating high performance of heterojunctions based on Cu_2S/CdS:Zn thin film.

References

[1] P. Priyadarshini, S. Das, R. Naik, RSC Advances **12**, 9599 (2022).
[2] M. Frumar, J. Jedelsky, B. Frumarov, T. Wagner, M. Hrdlicka, Journal of Non-Crystaline Solids **326327**, 399 (2003).
[3] W. A. Syed, S. Ahmed, M. S. Saleem, N. A. Shah, Chalcogenide Letters **12**, 215 (2015).
[4] J. Trolès, L. Brilland, Comptes Rendus Physique **18**, 19 (2017).
[5] A. Romeo, M. Terheggen, D. Abou Ras, D. L. Batzner, F .J. Haug, M. Kalin, D. Rudmann, A. N. Tiwari, Progress in Photovoltaics: Research and Applications **12**, 93 (2004).
[6] A. V. Feitosa, M. A. R. Miranda, J. M. Sasaki, M. A. Araujo-Silva, Brazilian Journal of Physics **34**, 656 (2004).
[7] J.-C. Lee, W. Lee, S.-H. Han, T. G. Kim,Y.-M. Sung, Electrochemistry Communications **11**, 231 (2009).
[8] T. Thongtem, A. Phurungrat, S. Thongtem, Journal of Materials Science **42**, 9316 (2007).
[9] Y. He, X. Yu, X. Zhao, Materials Letters **61**, 3014 (2007).
[10] W. Liang, M. H. Whangbo, Solid State Communications **85**, 405 (1993).
[11] Z. H. Han, Y. P. Li, H. Q. Zhao, S. H. Yu, Y. L. Yin, Y. T. Qian, Materials Letters **44**, 366 (2000).
[12] H. Moualkia, S. Hariech, M. S. Aida, Thin Solid Films **518**, 1259 (2009).
[13] Y. Rodríguez-Lazcano, H. Martínez, M. Calixto-Rodríguez, A. Núñez Rodríguez, Thin Solid Films **517**, 5951 (2009).
[14] R. A. Orozco-Terán, M. Sotelo-Lerma, R. Ramirez-Bon, M. A. Quevedo-López, O. Mendoza-González, O. Zelava-Angel, Thin Solid Films **343-344**, 587 (1999).
[15] P. K. Nair, M. T. S. Nair, Semiconductor Science and Technology **4**, 807 (1989).
[16] I. O. Oladeji, L. Chow, Thin Solid Films **474**, 77 (2005).
[17] Y. Wu, C. Wadia, W. Ma, B. Sadtler, A. P. Alivisatos, Nano Letters **8**, 2551 (2008).
[18] M. Saranya, C. Santhosh, S. Prathap Augustine, A. Nirmala Grace, Journal of Experimental Nanoscience **9**, 201 (2014).
[19] L. Soriano, M. Leon, F. Arjona, E. Garcia Camarero, Solar Energy Materials **12**, 149 (1985).
[20] Adel H. Omran Al-Khayatt, Mustafa D. Jaafer, Journal of Kufa – Physics **5**, 79 (2013).
[21] S. Lindroos, A. Arnold, M. Leskelä, Applied Surface

Science **158**, 75 (2000).
[22] M. Dhanasekar, G. Bakiyaraj, K. Rammurthi, International Journal of ChemTech Research **7**, 1057 (2015).
[23] R. S. Mane, C. D. Lokhande, Materials Chemistry and Physics **65**, 1 (2000).
[24] I. O. Oladeji, L. Chow, C. S. Ferekides, V. Viswanathan, Z. Zhao, Solar Energy Materials and Solar Cells **61**, 203 (2000).
[25] K. D. Dobson, I. Visoly-Fisher, G. Hodes, D. Cahen, Solar Energy Materials and Solar Cells **62**, 295 (2000).
[26] M. Courel, J. A. Andrade-Arvizu, O. Vigil-Galán, Solid-State Electronics **111**, 243 (2015).
[27] F. I. Ezema, D. D. Hile, S. C. Ezugwu, R. U. Osuji, P. U. Asogwa, Journal of Ovonic Research **6**, 99 (2010).
[28] A. Ashour, J. Optoelectron. Adv. M. **8**(4), 1447 (2006).
[29] E. Gaubas, I. Brytavskyi, T. Čeponis, J. Kusakovskij, G. Tamulaitis, Thin Solid Films **531**, 131 (2013).
[30] B. S. Munde, L. S. Ravangave, IOSR Journal of Applied Physics **9**, 50 (2017).
[31] M. Anbarasi, V. S. Nagarethinam, A. R. Balu, Materials Science - Poland **32**, 652 (2014).
[32] B. D. Cullity and S. R. Stock, Elements of X-Ray Diffraction, 3rd edn. Prentice Hall, 2001.
[33] P. K. Nair, O. G. Daza, A. A.-C. Reádigos, J. Campos, M. T. S. Nair, Semiconductor Science and Technology **16**, 651 (2001).
[34] L. Herissi, L. Hadjeris, M. S. Aida, J. Bougdira, Thin Solid Films **605**, 116 (2016).
[35] A. Mahdjoub, H. Moualkia, L. Remache, A. Hafid, Revue Algérienne de Physique **2**, 30 (2015).
[36] J. J. Tauc, Amorphous and Liquid Semiconductor, Plenum Press, New York, 1976.
[37] A. I. Oliva, J. E. Corona, R. Patiño, A. I. Oliva-Avilés, Bulletin of Materials Science **37**, 247 (2014).
[38] K. Usharani, A. R. Balu, G. Shanmugavel, M. Suganya, V. S. Nagarethinam, International Journal of Scientific Research and Reviews **2**, 53 (2013).
[39] D. Dutton, Physical Review **112**, 785 (1958).
[40] S. M. Sze, K. K. Ng, Physics of semiconductor devices, John Wiley & Sons, New York, 2006.
[41] J. Nomoto, K. Inaba, M. Osada, S. Kobayashi, H. Makino, T. Yamamoto, Journal of Applied Physics **120**, 125302 (2016).
[42] L. Isac, A. Duta, A. Kriza, S. Manolache, M. Nanu, Thin Solid Films **515**, 5755 (2007).
[43] S. B. Gadgil, R. Thangaraj, J. V. Iyer, A. K. Sharma, B. K. Gupta, O. P. Agnihotri, Solar Energy Materials **5**, 129 (1981).
[44] I. Luminit, P. Ionut, E. Alexandru, D. Anca, Energy Procedia **2**, 71 (2010).
[45] F. Ynineb, N. Attaf, M. S. Aida, J. Bougdira, Y. Bouznit, H. Rinnert, Thin Solid Films **628**, 36 (2017).
[46] A. H. Kacha, B. Akkal, Z. Benamara, M. Amrani, A. Rabhi, G. Monier, C. Robert-Goumet, L. Bideux, B. Gruzza, Superlattices and Microstructures **83**, 827 (2015).

*Corresponding author: labidi.herissi@univ-tebessa.dz